

# Kinetic analyses of thermally relativistic nonequilibrium flows

Ryosuke Yano and Kojiro Suzuki

*Dept. of Advanced Energy, Univ. of Tokyo, 5-1-5, Kashiwanoha, Kashiwa, Chiba, Japan*

**Abstract.** In this paper, we consider on the thermally relativistic nonequilibrium flows in the flat or curved spacetime. In the flat spacetime, the supersonic thermally relativistic flow around the prism is numerically analyzed using the Anderson-Witting model. Obtained numerical results show that the flowfield is remarkably different from that obtained by the Bhatnagar-Gross-Krook equation, which is the nonrelativistic limit of the Anderson-Witting model. Additionally, the sign of the dynamic pressure is opposite to that obtained by the Navier-Stokes-Fourier law on the basis of the Eckart decomposition. Finally, the thermally relativistic flow in the curved spacetime is numerically analyzed by solving the general relativistic Anderson-Witting model and the Einstein's equation simultaneously. In curved spacetime, nongravitational flow is induced owing to the local dependency of the equilibrium function on the local metric of curved spacetime. Such a flow is confirmed by the nongravitational initial cluster inside the stuffed black hole.

**Keywords:** Relativistic kinetic theory, Nonequilibrium flows

**PACS:** 95.30.Sf, 98.80.Jk, 51.10.+y

## INTRODUCTION

The relativistic hydrodynamics becomes so significant in the field of the high energy physics. In particular, the necessities of the theoretical descriptions on the experimental results via the RHIC (Relativistic Heavy Ion Collider) are enhanced. For example, the behavior of the Quark-Gluon Plasma must be analyzed by solving Wong-Boltzmann equation coupled to the Yang-Mills equation [1]. On the other hand, the relativistic hydrodynamics is not established yet due to some unsolved problem. One is the incomplete decomposition method. The other is the problem of the causality, which is caused by the diffusion term in the relativistic Navier-Stokes-Fourier (NSF) equation, whereas the problem of the causality is not involved in the relativistic Boltzmann equation. As the most classic decomposition, the Eckart decomposition [2] is well known. On the other hand, Kunihiro et al. [3] show that the Eckart decomposition is not complete formalism, when we introduce the relativistic NSF equation. However, the Israel-Stewart equation [4], which replaces parts of the heat flux and the pressure deviator in the NSF equation by Grad's moment equation to avoid the problem of the causality, includes the problem of propagation limit involved in the Grad's moment equations. To avoid some troublesome problems involved in the relativistic hydrodynamic equation, we focus on the Anderson-Witting (A.W.) model [5][6], which is the reduced model of the relativistic Boltzmann equation. Conserved quantities, the number density, velocity and temperature, which are needed to determine the relativistic equilibrium function namely Maxwell-Jüttner function [5], can be correctly decomposed via the Eckart decomposition. Then, thermally relativistic nonequilibrium flows in the flat or curved spacetime are analyzed using the A.W. model. Thermally relativistic state is characterized by  $0 < \zeta = mc^2/(k\theta) \leq 100$ , in which  $m$  is the mass of a particle,  $c$  is the speed of light,  $k$  is the Boltzmann constant and  $\theta$  is the temperature. As an object of analysis, the supersonic thermally relativistic flow around the prism, which includes hydrodynamically interesting problems such as the shock, expansion, boundary layer and vortex, is considered. The numerical result obtained by the A.W. model is compared with that obtained by the Bhatnagar-Gross-Krook (BGK) model [5], which is the nonrelativistic limit of the A. W. model. The differences between the numerical results obtained by the A. W. model and those obtained by the BGK model are remarkable, when we compare the profiles of the number density and temperature along the stagnation streamline (SSL) obtained by both of models. The sign of the dynamic pressure is opposite to that obtained by the NSF law. Such an abnormal profile of the dynamic pressure obtained by the A. W. model implies the insufficiency of the Eckart decomposition. As an extension to the general relativistic flows, the thermally relativistic flow in the curved spacetime is numerically analyzed by solving the nongravitational initial cluster inside the stuffed black hole. Such a nongravitational cluster is described by the dependency of the general relativistic Maxwell-Jüttner function on the local metric of the curved spacetime. Here, the Einstein's equation is solved using the Z4 formalism [7] by coupling to the general relativistic A.

W. model.

## ANDERSON-WITTING MODEL

In this section, the A. W. model is revisited. For the general expression, the general relativistic A. W. model is discussed, because the A. W. model in flat spacetime is the special case of the general relativistic A. W. model.

The general relativistic Boltzmann equation with the distribution function based on four-momentum  $p^\mu$  is written as: [5]

$$p^\mu \frac{\partial f}{\partial x^\mu} - \Gamma_{\mu\nu}^i p^\mu p^\nu \frac{\partial f}{\partial p^i} = L[f],$$

$$L[f] = \frac{U_L^\mu p_\mu}{c^2 \mathcal{S}} \left( f^{(0)} - f \right) \left( \text{where } f^{(0)}(x^\mu, p^\mu) = \frac{n}{4\pi m^2 c k \theta K_2(\zeta)} e^{-\frac{U^\mu p_\mu}{k\theta}} \right), \quad (1)$$

where  $f$  is the distribution function defined by  $f \equiv f(x^\mu, p^i)$ , ( $i = 1, 2, 3$ ),  $\Gamma_{\mu\nu}^i$  is the Christoffel symbol,  $f^{(0)}$  is the Maxwell Jüttner function, and  $K_2(\zeta)$  is the modified Bessel function of the second kind. In numerical analysis, the treatment of momentum space is difficult, because  $p^\mu$  approaches infinity as the velocity of particles approaches the speed of light.  $\mathcal{S}$  in eq. (1) is defined by:

$$\mathcal{S} = \frac{1}{4n\pi\sigma v_s} \left( \text{where } v_s = \sqrt{\frac{\zeta^2 + 5\mathcal{G}\zeta - \mathcal{G}^2\zeta^2}{\mathcal{G}(\zeta^2 + 5\mathcal{G}\zeta - \mathcal{G}^2\zeta^2 - 1)} \frac{k\theta}{m}} \right), \quad (2)$$

where  $\mathcal{G} \equiv K_3(\zeta)/K_2(\zeta)$ , in which  $K_3(\zeta)$  is the modified Bessel function of the third kind, and  $\sigma$  is the total cross section of the collision [5].  $U_L^\mu$  in eq. (1) is the four-velocity of the flow defined by Landau-Lifshitz as [5]

$$U_L^\mu = U^\mu + \frac{q^\mu}{ne + p}, \quad (3)$$

where  $p$  is the static pressure defined as  $p = nk\theta$ ,  $q^\mu$  is the four-heat flux and  $e$  is the energy density.

As a result of eq. (1), the accurate numerical integration of the distribution function in momentum space becomes difficult when the number of particles with velocity near the speed of light is nonnegligible. The use of velocity space instead of momentum space as the phase space of the distribution function is therefore expected to yield a more accurate integration of the distribution function, because the velocity space is bounded by the metric [5]. For accurate integration, we must therefore derive the general relativistic Boltzmann equation on the basis of the velocity space instead of the momentum space, namely,  $f(x^\mu, p^i) \rightarrow f(x^\mu, v^i)$ .

The Liouville law gives the following relation for the distribution function:

$$\frac{df(x^\mu(\tau^*), v^i(\tau^*))}{d\tau^*} = \frac{\partial f}{\partial x^\mu} \frac{dx^\mu}{d\tau^*} + \frac{\partial f}{\partial v^i} \frac{dv^i}{d\tau^*}, \quad (4)$$

Here,  $\tau^* = \tau/m$ , where  $\tau$  is the proper time and  $m$  is the mass of a particle.

To derive  $dv^i/d\tau^*$ , we use the equation of motion of a particle under a gravitational field:

$$\frac{dp^i}{d\tau^*} = -\Gamma_{\mu\nu}^i p^\mu p^\nu = \Gamma(v) \frac{d\Gamma(v)v^\mu}{dt} = -\Gamma_{\mu\nu}^i \Gamma(v)^2 v^\mu v^\nu, \quad \left( \text{where } p^\mu \equiv \frac{dx^\mu}{d\tau^*} \right), \quad (5)$$

where  $\Gamma(v)$  is defined as follows by using a (3+1) ADM system [7] with the lapse  $\alpha$ , intrinsic curvature  $\gamma_{ij}$ , and zero shift  $\beta^i = 0$  [7]:

$$\Gamma(v) \equiv \frac{dt}{d\tau} = \frac{1}{\sqrt{\alpha^2 - \hat{v}^2}}, \quad \left( \text{where } v^i = \frac{dx^i}{dt}, \quad \hat{v}^2 \equiv \gamma_{ij} v^i v^j / c^2 \right). \quad (6)$$

From eq. (6),  $\hat{v} < \alpha$ , and thus  $\psi^i = dv^i/dt$  is defined as

$$\psi^i = \frac{dv^i}{dt} = \mathcal{Q}v^i - \mathcal{C}^i + \frac{v^i}{\alpha^2} \mathcal{R}_j \mathcal{C}^j \left( \text{where } \mathcal{C}^i = \Gamma_{\mu\nu}^i v^\mu v^\nu \wedge \mathcal{R}_j = \gamma_{jk} v^k \wedge \mathcal{Q} = \mathcal{S} + \sum_{i,j=1}^3 \gamma_{ij} \mathcal{S}_{ij} \right), \quad (7)$$

where  $\mathcal{S}$  and  $\mathcal{S}_{ij}$  in eq. (7) are defined as

$$\mathcal{S} \equiv \partial_t \alpha, \quad \mathcal{S}_{ij} \equiv \partial_t \gamma_{ij}. \quad (8)$$

Substituting eq. (7) into eq. (4) yields the general relativistic A. W. model based on the velocity space: [8]

$$\frac{\partial f}{\partial t} + v^i \frac{\partial f}{\partial x^i} + \psi^i \frac{\partial f}{\partial v^i} = \frac{1}{\Gamma(v)} L[f]. \quad (9)$$

The first and second moments,  $N^\mu$  and  $T^{\mu\nu}$ , are obtained by evaluating [5]

$$N^\mu = c \int_{\mathcal{R}^3} p^\mu f \sqrt{g} \frac{d^3 p}{p_0}, \quad T^{\mu\nu} = c \int_{\mathcal{R}^3} p^\mu p^\nu f \sqrt{g} \frac{d^3 p}{p_0}, \quad (10)$$

where  $c$  is the speed of light in the Minkowski metric and  $g \equiv \det(g_{\mu\nu})$ , in which  $g_{\mu\nu}$  is the metric tensor.

Rewriting eq. (10) with momentum space  $\mathcal{R}^3$  replaced by velocity space  $\mathcal{V}^3$  yields the following:

$$N^\mu = m^3 c \int_{\mathcal{V}^3} \Gamma(v)^5 v^\mu f \sqrt{g} d^3 \mathbf{v}, \quad T^{\mu\nu} = m^4 c \int_{\mathcal{V}^3} \Gamma(v)^6 v^\mu v^\nu f \sqrt{g} d^3 \mathbf{v}. \quad (11)$$

The Eckart decomposition [2] yields the projected moments, number density  $n$ , pressure deviator  $p^{<\mu\nu>}$ , static pressure  $p$ , dynamic pressure  $\bar{\omega}$ , and energy per particle  $e$  as follows: [2] [5]

$$n = \frac{1}{c^2} N^\nu U_\nu, \quad p^{<\mu\nu>} = \left( \Delta_\gamma^\mu \Delta_\delta^\nu - \frac{1}{3} \Delta^{\mu\nu} \Delta_{\gamma\delta} \right) T^{\delta\gamma}, \quad p + \bar{\omega} = -\frac{1}{3} \Delta_{\mu\nu} T^{\mu\nu},$$

$$q^\mu = \Delta_\gamma^\mu U_\nu T^{\nu\gamma}, \quad e = \frac{1}{nc^2} U_\mu T^{\mu\nu} U_\nu, \quad (12)$$

where  $U^\mu = \Gamma(u) u^\mu$ , in which  $u^\mu = (c, u^i)$ ,  $u^i$  is the flow velocity of the  $i$ -th component and  $\Gamma(u) = 1/\sqrt{\alpha^2 - \gamma_{ij} u^i u^j}/c^2$ , and where  $U_\mu = \Gamma(u) u_\mu$ , in which  $u_\mu = (\alpha^2 c, -u^j \gamma_{ij})$  is the covariant four velocity of the flow [2]. The projector  $\Delta_{\mu\nu}$  is defined as [2] [5]

$$\Delta_{\mu\nu} = g_{\mu\nu} - \frac{U_\mu U_\nu}{c^2}. \quad (13)$$

## THERMALLY RELATIVISTIC NONEQUILIBRIUM FLOW IN FLAT SPACETIME

In this section, the thermally relativistic flow in the flat spacetime, namely  $g_{\mu\nu} = \eta_{\mu\nu} = (1, -1, -1, -1)$ , is considered. To discuss the obtained numerical results in the framework of the NSF law via the Eckart decomposition, the relativistic NSF law in flat spacetime is written as follows [5]:

$$\bar{\omega} = -\eta \nabla_\alpha U^\alpha, \quad (14)$$

$$p^{<\alpha\beta>} = 2\mu \left[ \frac{1}{2} \left( \Delta_\gamma^\alpha \Delta_\delta^\beta + \Delta_\delta^\alpha \Delta_\gamma^\beta \right) - \frac{1}{3} \Delta^{\alpha\beta} \Delta_{\gamma\delta} \right] \nabla^\gamma U^\delta, \quad (15)$$

$$q^\alpha = \lambda \left( \nabla^\alpha \theta - \frac{\theta}{nh_E} \nabla^\alpha p \right), \quad (16)$$

where  $\eta$  is the bulk viscosity,  $\mu$  is the viscosity coefficient,  $\lambda$  is the thermal conductivity and  $h_E = ne + p$ .

As an object of analysis, the supersonic thermally relativistic flow around the prism, which includes hydrodynamically interesting problems such as the shock, expansion, boundary layer and vortex, is considered. The numerical result obtained by the A.W. model is compared with that obtained by the Bhatnagar-Gross-Krook (BGK) model, which is the nonrelativistic limit of the A. W. model. For easier comprehension of physical conditions, for the observer's frame the absolute standard of rest is used as the hypothetical inertial frame. We use  $(x, y, z)$  instead of  $(x^1, x^2, x^3)$  and  $(v^x, v^y, v^z)$  instead of  $(v^1, v^2, v^3)$ . The velocity corresponding to uniform flow is  $u^x = 0.6c$ ,  $u^y = 0$ ,  $u^z = 0$ . The temperature of the uniform flow is  $\theta_\infty = mc^2/45k$  ( $\zeta_\infty = 45$ ). Under these conditions, the Mach number of uniform flow calculated from eq. (2) is 3.247 ( $\cdot: v_s = 0.185317c$ ). The temperature of the wall is  $\theta_w = mc^2/30k$  ( $\zeta_w = 30$ ) and the complete diffusive

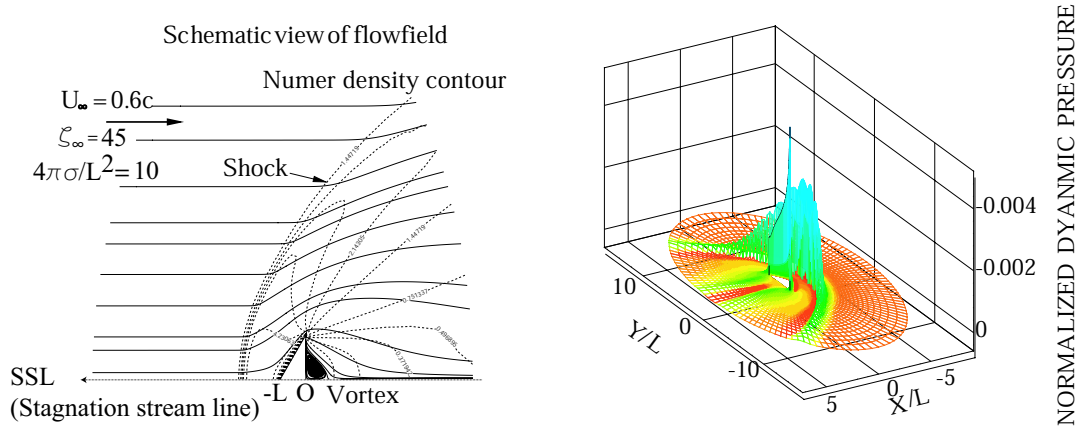


**FIGURE 1.** Schematic view of the flowfield (Left) and bird's eye view of the profile of the dynamic pressure (Right).

wall is used. In eq. (2),  $4\pi\sigma/L^2 = 10$ . Molecules are all assumed to be monatomic hard-sphere molecules. For the numerical grid,  $(v^x, v^y, v^z, x, y) = (64, 64, 64, 125, 60)$ . Figure 1 shows the schematic view of the flowfield in its left side (Left) and bird's eye view of the profile of the dynamic pressure on  $x-y$  plane in its right side (Right). As shown in Fig. 1 (Left), the vertex angle of the prism is 120 degrees. The dynamic pressure in Fig. 1 (Right) is remarkable inside the shock structure and near the wall, and the sign of the dynamic pressure is opposite to that approximated by the NSF law in eq. (14). Such an abnormal behavior of the dynamic pressure implies the insufficiency of the Eckart decomposition. The BGK model is solved using the same Mach number to clarify the relativistic effects such as the Lorentz contract [5] or the thermally relativistic effect [6], which changes thermodynamic properties of matters as  $0 < \zeta \leq 100$ . Figure 2 (Left) shows profiles of the number density and temperature along SSL obtained by the A. W. and BGK models. As shown in Fig. 2 (Left), there are remarkable differences between profiles obtained by the A. W. model and those obtained by the BGK model. The number density and temperature behind the shock obtained by the A. W. model are higher than those obtained by the BGK model, because fluxes of the number density, momentum and energy increase owing to the decrease of the volume by the Lorentz contract. In the low velocity regime such as thermally boundary layer behind the shock, thermally relativistic effects are significant, because the  $\zeta_{min} \simeq 5.7$  behind the shock is enough small to change thermodynamic properties of matters. Actually, there are remarkable differences between profiles of the number density and temperature in the thermally boundary layer obtained by the A. W. model and those obtained by the BGK model. Figure 2 (Right) shows profiles of heat flux  $q^x$  along the stagnation streamline.  $q^x$  is approximated from eq. (16) by using the N.S.F law. From the spatial gradient of  $\theta$  and  $p$ ,  $(q^x)_{NSF}$  approximated by the NSF law is introduced from eq. (16). We define the heat flux by the gradient of the temperature as  $(q_t^x)_{NSF} = \lambda \nabla^\alpha \theta$  and by the gradient of the static pressure as  $(q_p^x)_{NSF} = -\lambda \frac{\theta}{nh_E} \nabla p$ . As a result,  $(q^x)_{NSF} = (q_t^x)_{NSF} + (q_p^x)_{NSF}$ . For results from the A. W. model, Figure 2 (Right) shows  $(q^x)_{NSF}$  together with  $q^x$  along the stagnation streamline on the left  $y$  axis, and on the right  $y$  axis, Fig. 2 (Right) shows  $|(q_p^x)_{NSF} / (q_t^x)_{NSF}|$  along the stagnation streamline, which is the ratio of absolute values of  $(q_t^x)_{NSF}$  and  $(q_p^x)_{NSF}$ . The thermal conductivity  $\lambda$  from the A. W. model, which is necessary for the calculation of  $(q^x)_{NSF}$ ,  $(q_t^x)_{NSF}$  and  $(q_p^x)_{NSF}$ , is given by [5]. As shown in Fig. 2 (Right),  $q^x \leq (q^x)_{NSF}$  near  $2.4 \leq -X/R \leq 3.0$  in the shock structure indicates significant effects by the terms from the Burnett equation. Near  $-X/R \simeq 1.4$ ,  $|(q_p^x)_{NSF} / (q_t^x)_{NSF}|$  exhibits a maximum value. As shown in Fig. 2 (Right), the heat flux calculated by the gradient of the isotropic pressure,  $(q_p^x)_{NSF}$ , is nonnegligible for the calculated heat flux  $q^x$  in this problem.

## THERMALLY RELATIVISTIC NONEQUILIBRIUM FLOW IN CURVED SPACETIME

The flow in the curved spacetime is induced exclusively by the gravitational force, which is revealed by the term  $\psi^i \partial f / \partial v^i$  in eq. (9), when particles are thermally nonrelativistic (i.e.,  $10^2 \ll \zeta$ ). When particles are thermally relativistic (i.e.,  $1 < \zeta < 10^2$ ) or thermally ultrarelativistic (i.e.,  $(\zeta \leq 1)$ ), however, the flow in curved spacetime is also induced by gravitational-force-free particle motion, which is revealed by the term  $v^i \partial f / \partial x^i$  in eq. (9). This nongravitational thermally relativistic flow is caused by the dependence of the equilibrium function, or the so-called

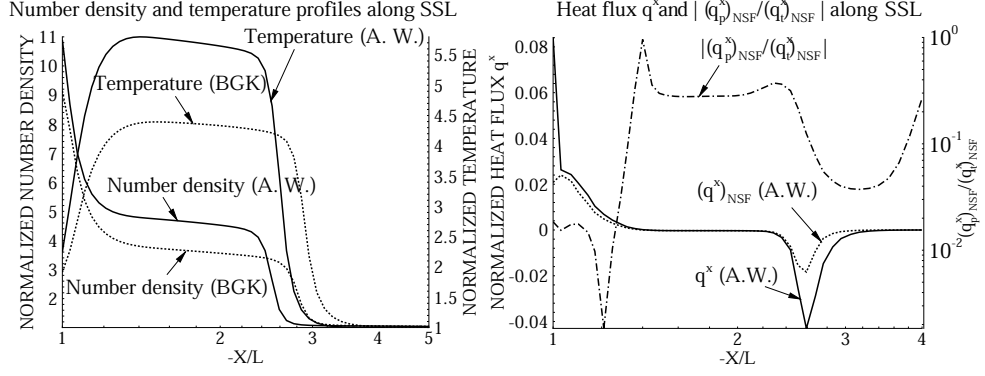


**FIGURE 2.** Profiles of number density and temperature along SSL (Left), and  $q^x$  and  $|(q_p^x)_{NSF}/(q_l^x)_{NSF}|$  along SSL (Right).

Maxwell-Jüttner function [5], on the local lapse and intrinsic curvature. As an object of analysis, we consider on the nongravitational initial cluster inside the stuffed black hole. A stuffed black hole [7] is a black hole whose inward spacetime of the Schwarzschild radius,  $R_s$ , is described using the FRW (Friedmann-Robertson-Walker) metric in the closed case and whose outward spacetime is described using the Schwarzschild metric. The particles inside  $R_s$  are uniformly distributed. Here, we consider a stuffed black hole that has relativistic thermal energy. The initial gauge condition of a thermally relativistic stuffed black hole in isotropic coordinates [7] is

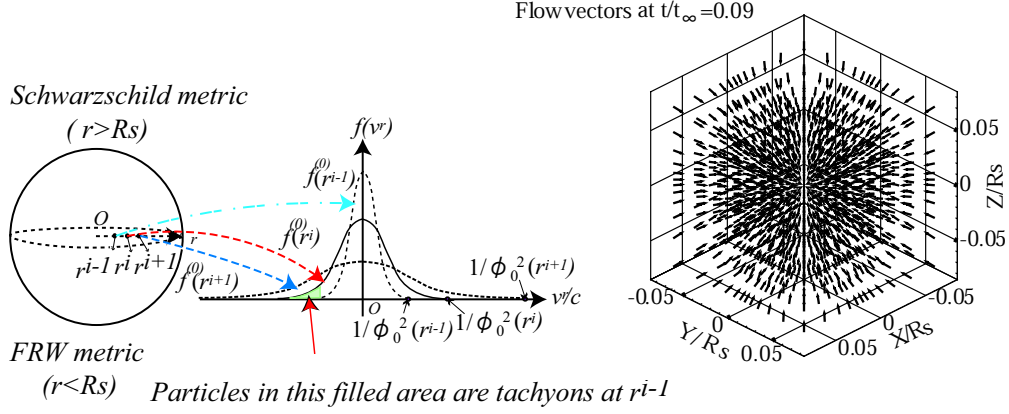
$$\alpha_0 = 1, \quad \gamma_{ij,0} = \delta_{ij}\phi_0^4, \\ \text{if } r < R_s, \quad \phi_0^4 = 64 \left\{ 1 + \left( \frac{2rc^2}{MG} \right)^2 \right\}^{-2}, \quad \text{if } r > R_s, \quad \phi_0^4 = \left( 1 + \frac{MG}{2rc^2} \right)^{-4}, \quad r = \sqrt{x_1^2 + x_2^2 + x_3^2}, \quad (17)$$

where the subscript "0" indicates the initial state,  $M$  is the mass of the black hole,  $G$  is the gravitational constant,  $\delta_{ij}$  is Kronecker's delta function, and  $R_s$  is given by

$$R_s = \frac{MG}{2c^2} = \frac{1}{8} \sqrt{\frac{3c^4}{2\pi\tau_0 G}}, \quad \tau_0 = T^{00}|_{t=0}, \quad (18)$$

where  $\tau$  is the energy density.

To simplify the analytical discussion, we use a spherically symmetric distribution function,  $f(t, r, v^r) = f(t, r, v^r, \vartheta, \varphi)$ , because  $f(t, r, v^r, \vartheta, \varphi)$  is spherically symmetric owing to the spherical symmetry of the FRW metric and is uniform in the directions of  $\vartheta$  and  $\varphi$ , where the Cartesian coordinates  $(x^1, x^2, x^3)$  are converted into spherical coordinates  $(r, \vartheta, \varphi)$  via the relations  $(x^1, x^2, x^3) = (r \sin \vartheta \cos \varphi, r \sin \vartheta \sin \varphi, r \cos \vartheta)$  and  $(v^1, v^2, v^3) = (v^r \sin \vartheta \cos \varphi, v^r \sin \vartheta \sin \varphi, v^r \cos \vartheta)$ , in which  $0 \leq \vartheta < \pi/2$  and  $0 \leq \varphi < \pi$ . Assuming that the number density is uniform (i.e.,  $n = n_\infty$ ), that the flow velocity is zero, and that the temperature is uniform (i.e.,  $\theta = \theta_\infty$ ), then from eqs. (1) and (17), the initial equilibrium distribution function is  $f^{(0)} = n_\infty / (4\pi m^2 c k \theta_\infty K_2) e^{-\zeta_\infty / \sqrt{1 - \phi_0^4 (v^r)^2 / c^2}}$ , where  $\zeta_\infty = mc^2 / (k\theta_\infty)$ . Figure 3 (Left) shows the initial state of the distribution function for three points,  $i-1$ ,  $i$  and  $i+1$ , along the radial axis  $r$ , where  $r_{i-1}, r_i, r_{i+1} < R_s$ . This figure reveals that the shape of the distribution function for each of these three points,  $f^{(0)}(0, r^{i-1}, v^r)$ ,  $f^{(0)}(0, r^i, v^r)$  and  $f^{(0)}(0, r^{i+1}, v^r)$ , depends on  $\gamma_{ij}$  given by eq. (17) from eq. (1). Here, we consider  $f(\Delta t, r^i, v^r)$ , where  $\Delta t \ll 1$ . For this case, the negative velocity tail of  $f^{(0)}(0, r^{i+1}, v^r)$ , which inflows into the negative tail of  $f^{(0)}(\Delta t, r^i, v^r)$ , is higher than that of  $f^{(0)}(0, r^i, v^r)$ , whereas the positive velocity tail of  $f^{(0)}(0, r^{i-1}, v^r)$ , which inflows into the positive tail of  $f^{(0)}(\Delta t, r^i, v^r)$ , is lower than that of  $f^{(0)}(0, r^i, v^r)$ . During  $\Delta t$ , the number of particles inflowing from  $r^{i+1}$  into  $r^i$  with the negative  $v^r$  is higher than that inflowing from  $r^{i-1}$  into  $r^i$  with the positive  $v^r$ . Consequently,  $f(\Delta t, r^i, -|v^r|) > f(\Delta t, r^i, |v^r|)$ , thus leading to a negative flow velocity, which is equivalent to the cluster of a particle into the origin, namely, the center of the black hole. Slicing parameters are determined to yield the constant local maximum speed  $c/\phi_0^2$  to avoid the numerical formation of tachyons, which is indicated by the inflow of particles in the shaded domain of  $f^{(0)}(0, r^i, v^r)$  into  $r^{i-1}$  in Fig. 3 (Left). In the presence of particle collisions, such a cluster is confirmed numerically by simultaneously solving the nongravitational general relativistic



A. W. model and Einstein's equation based on the Z4 formalism. The nongravitational general relativistic A. W. model indicated by  $\psi^i = 0$  in eq. (9). For numerical analysis, we consider only the cubic domain  $|x|, |y|, |z| \leq R_s/10$ . The number density, velocity, temperature and gauge variables of the Z4 formalism at the boundary are fixed at their initial values. Once particles and gauge variables move from the calculated cubic domain to the outer boundary, they never return to the calculated cubic-domain. Namely, the nonreflecting boundary condition is used. For the numerical grid, we use the Cartesian grid,  $(x, y, z, v^x, v^y, v^z) = (39, 39, 39, 48, 48, 48)$  First, we nondimensionalize the macroscopic physical quantities and set  $G/c^2 = 1/(n_\infty m L_\infty^2)$ , where  $L_\infty$  is a representative length. Then, we set the normalized initial macroscopic quantities as  $n/n_\infty = 1$ ,  $\zeta_\infty = mc^2/(k\theta_\infty) = 45$  and  $u^i/c = 0$ , and define the initial energy density  $\tau_0$  in eq. (18) as  $\tau_{0,\infty}/(n_\infty mc^2) = 1.032$ , which yields  $R_s/L_\infty = 0.085$  from eq. (18), and  $4\pi\sigma/L_\infty^2 = 10$  in eq. (2). The initial conditions of the lapse  $\alpha$  and intrinsic curvature  $\gamma_{ij}$  are given by eq. (17). Einstein's equation is then modified using the results estimated using the nongravitational general relativistic A. W. model [8]. Figure 3 (Right) shows the flow vectors at  $t/t_\infty = 0.09$  and numerically confirms the cluster at the origin as predicted by analytical discussions.

## CONCLUSIONS

In this paper, we considered on the thermally relativistic flows in the flat or curved spacetime by solving the A. W. model. From obtained numerical results in the case of the flat spacetime, the abnormal behavior of the dynamic pressure implies the insufficiency of the Eckart decomposition. Additionally, the contribution of the gradient of the pressure to the heat flux is nonnegligible. From obtained numerical results in the case of the curved spacetime, the nongravitational thermally relativistic flow induced by the local gradient of the metric of the curved spacetime exists inside the stuffed black hole, because the local equilibrium function depends on the local metric of the curved spacetime.

## REFERENCES

1. B. Schenke, Jet evolution in Yang-Mills-Wong simulations, Nuclear Phys. A, Vol. 830, 1-4, pp689-692 (2009).
2. C. Eckart, The thermodynamics of irreversible process, III. Relativistic theory of a simple fluid, Phys. Rev. 58, pp919-924 (1940).
3. T. Kunihiro, Y. Minami and K. Tsumura, Critical Opalescence around the QCD Critical Point and Second-order Relativistic Hydrodynamic Equations Compatible with Boltzmann Equation, Nuclear Phys. A, Vol. 830, 1-4, pp207-210 (2009).
4. J. M. Stewart, *Non-equilibrium relativistic kinetic theory*, Lecture notes in Phys. Vol. 10, Springer, Heidelberg (1971).
5. C. Cercignani and G. Kremer, *The relativistic Boltzmann Equation: Theory and Applications*, Progress in Math. Phys., Vol. 22, Springer-Verlag (2002).
6. R. Yano, K. Suzuki and H. Kuroda, Numerical analysis of relativistic shock layer problem by using relativistic Boltzmann-kinetic equations, Physica A, Vol. 381, pp8-21 (2007).
7. A. Arbona, C. Bona, J. Carot, L. Mas, J. Masso and J. Stela, Phys. Rev. D 57, 2397 (1998).
8. R. Yano, K. Suzuki and H. Kuroda, Phys. Rev. D, 80, 123506 (2009).